C.P. No. 445
(20,175)
A.R.C. Technical Report

C.P. No. 445
(20,175)
A.R.C. Technical Report

MINISTRY OF SUPPLY

AERONAUTICAL RESEARCH COUNCIL

CURRENT PAPERS

A One - Dimensional Theory of Liquid - Fuel Rocket Combustion

By

D.B. Spalding,
Imperial College, London

LONDON: HER MAJESTY'S STATIONERY OFFICE

1959

FOUR SHILLINGS NET

ERRATA

Page 3 — Insert at bottom of page "τ = reactedness.

Page 9 — Equation (36). The last bracket $(1 - \zeta^S)$ should be $(1 - \zeta^5)$.

Page 13 — Equation (50). Insert brackets and $\frac{1}{2}$ i.e.,

$$f_1 = 1 + 0.245 \{Re_o . |\omega - \chi| . \zeta\}^{\frac{1}{2}}.$$

C.P.No.445

A One-Dimensional Theory of Liquid-Fuel Rocket Combustion

- By -
D. B. Spalding,
Imperial College, London

19th May, 1958

SUMMARY

The system considered is an ideal rocket motor in which all properties depend only on distance from the injector face and droplets have uniform diameter on entry. Processes considered are droplet drag, vaporization and chemical reaction. Equations are derived, integration of which leads to a prediction of the minimum length of rocket motor. Such predictions are made for the particular case in which the chemical reaction rate is high and the fuel and oxidant, though injected separately, have similar droplet properties. Calculations are made of the effects of droplet size, droplet injection velocity, final gas velocity, droplet transfer number, and other variables. The mean residence time, and the concentration-time curve of an injected tracer, are also calculated.

1. Introduction

1.1 Purpose of the paper

Much is known about the burning of single droplets, but this knowledge appears not to have been applied quantitatively to combustion in liquid-fuel rocket motors.

The present report represents such an application, which is intended ultimately to lead to:-

(i) an assessment of how far actual rocket performance can be quantitatively explained in terms of simple physical and chemical idealisations of the actual processes;

(ii) the disclosure of what fundamental data are needed for the understanding of rocket combustion and what are not necessary;

(iii) guiding principles for the assistance of rocket motor designers.

1.2/

1.2 Method

The paper is entirely theoretical, and involves the investigation of an ideal rocket motor, the main feature of which is that droplet and gas conditions are supposed to depend only on distance from the injector face; i.e., the model is one-dimensional. Both bi-propellant and mono-propellant systems can be considered in this way.

Assumptions, based on small-scale experiments, are made for:

(i) the law of droplet vaporization

(ii) the law of droplet drag

(iii) the law of chemical reaction rate.

Mathematical analysis then permits prediction of the variation of gas and droplet states along the length of the combustion chamber. In particular the length necessary for complete combustion can be evaluated.

1.3 General remarks

It will be shown that in a simple case (Model Ia) an analytical solution is possible. In more complicated cases, numerical methods and high-speed computing machinery are required, but the solution procedure is still relatively straightforward.

Use of the results of the theory requires data about:-

(i) the size and velocity of droplets produced by the injector,

(ii) the thermodynamic properties of the propellants,

(iii) the chemical reaction rates in the propellant gases.

Some of these data are available, but it is hoped that the present work will stimulate the collection and measurement of more.

Only when these data have been inserted in the theoretical solutions can the value of the theoretical models be assessed thoroughly. However it appears that qualitatively the implications of the theory are realistic.

2. The One-Dimensional Idealisation

2.1 Nature of the theoretical model

Consider the liquid-fuel rocket motor shown in Fig. 1. It is supposed that droplets of uniform size and uniform velocity are injected through the injector and travel to the right. No distinction is made between oxidant and propellant droplets, although this could be done with a relatively small extension of the theory. (Consideration of injected sprays of non-uniform size and velocity is also possible, but involves a major increase in the amount of computation.) Fig. 2 shows the expected trends.

The droplets decrease continuously in diameter during their travel, as a result of vaporization. The mass flow rate of gas therefore increases from zero at the injector plane to a maximum at the

plane/

plane where the droplets finally disappear. The relation between gas velocity and droplet size is easily determined from the mass-conservation principle.

The droplets are injected at a finite velocity and at first are slowed down by friction with the gas. Later however the gas velocity begins to exceed the droplet velocity as a consequence of vaporization and combustion; the droplets therefore tend to be accelerated once more.

The state of the gas can vary between that of unreacted propellant vapour at the droplet temperature and that of combustion products in equilibrium. The extent of the approach to equilibrium depends on the rate of chemical reaction. This rate depends on the instantaneous state of the gas, i.e., primarily on the local fuel-oxidant ratio and reactedness.

It is assumed that the process is steady, that heat transfer to the duct walls is negligible, that turbulent mixing in a longitudinal direction is absent, and that the kinetic energies of motion are small.

2.2 The law of droplet vaporization

The rate of decrease of droplet radius depends only on the instantaneous state of the droplet, the local gas state, and the relative velocity of droplet and gas. If the rocket is a bi-fuel one, chemical reaction rates scarcely influence the rate of vaporization; mono-propellant droplet vaporization rates are affected by chemical reactivity however, at least for large droplets and large reaction rates[1].

It is usually possible to write the law of droplet vaporization as

$$\frac{Dr}{Dt} = v\frac{dr}{dx} = -\sigma(\tau).R(r).f_1(Re) \qquad \ldots(1)$$

where r = droplet radius

D/Dt = substantial derivative

v = droplet velocity

x = axial distance

σ = function of reactedness, τ, = 1 for gas in equilibrium

R = function of radius alone

= $(1/r)(k/c\rho_\ell)\,\ell n(1 + B)$ in simple cases (Ref. 1)

k = average gas conductivity

c = average gas specific heat

ρ_ℓ = droplet density

B = transfer number

f_1 = function of droplet Reynolds number.

It/

It is possible to take account, in the function R, of transient effects within the droplet, and of chemical reaction around the droplet. R is therefore a known function, as is σ also.

2.3 The law of droplet drag

The rate of change of droplet velocity depends on its mass and on its drag. The relation can be written as

$$v \frac{dv}{dx} = \frac{9}{2} \frac{\mu_g}{\rho_\ell r^2} (u - v).m(\tau).f_2(Re) \qquad ...(2)$$

where

μ_g = viscosity of gas in equilibrium state

m = function of τ expressing variation of gas viscosity with temperature, = 1 if τ = 1

f_2 = function of droplet Reynolds number.

For small Re, f_2 = 1; equation (2) reduces to Stokes's Law. As the Reynolds number increases, f_2 rises above unity. This is discussed in Section 6.1. A modification to (2) may be made to account for the fact that the outward mass transfer from the droplet surface tends to reduce the drag (see Section 5.1).

2.4 The law of chemical reaction rate

For mono-propellant droplets, chemical reaction rate influences R, as already indicated. Ref. 1 gives details of this influence for the case in which the bulk of the gas can be regarded as in equilibrium.

When the reaction rate is sufficiently low, for either mono-propellant or bi-propellant systems, the gas stream reactedness is not unity. It is then necessary to take account of the way in which the reaction rate depends on reactedness (we assume for simplicity that the fuel-oxidant ratio of the gas stream is uniform; the more general case can also be dealt with).

Knowledge of chemical kinetics is insufficient to warrant more than the assumption of the law

$$\dot{q}''' = \dot{q}'''_m.\psi(\tau) \qquad ...(3)$$

where

$\dot{q}'''$ = volumetric energy release rate,

$\dot{q}'''_m$ = maximum value of $\dot{q}'''$, a function of the propellant composition, its pressure, and its initial temperature,

ψ = function of reactedness.

[N.B. Equation (3) is U.H.T. 4 of Ref. 2. See, for example, Ref. 3 for discussion.]

2.5/

2.5 Differential equations: physical terms

Mass conservation in droplet vaporization:

$$G = \rho_g u.\delta(\tau) + G\, r^3/r_o^3 \qquad \ldots(4)$$

where G = mass flow rate of injected material per unit duct area

ρ_g = density of gas in equilibrium

u = gas velocity

δ = function of τ expressing dependence of gas density on reactedness

r = local droplet radius

r_o = droplet radius at injection.

Steady-flow energy equation:

For an elementary control volume enclosing the gas stream, we have

$$u\, c\, \rho_g\, \delta \frac{d\tau}{dx} - 3\, c\, \tau\, G \frac{r^2}{r_o^3}\frac{dr}{dx} = \frac{\dot{q}'''_m}{(T_b - T_u + \frac{Q}{c})}.\psi \qquad \ldots(5)$$

where T_b = equilibrium (burned) gas temperature

T_u = temperature of newly-formed vapour

Q = heat transfer to droplet to vaporize unit mass.

In addition we have the differential equations (1) and (2).

2.6 Preliminary remarks about the solution

The differential equations, together with knowledge about the size and velocity of the injected droplets and the properties of the substances, enable the conditions throughout the rocket motor to be calculated without difficulty.

Even without performing the computations, it is possible to see that the solution must yield curves of the general shape sketched in Fig. 2. This shows the steady decrease in droplet diameter, the steady rise of the gas velocity, and the initial decrease and subsequent increase of the droplet velocity. A quantity of great interest is x^*, the axial distance at which the droplets finally disappear; for clearly the rocket chamber should not be shorter than this length.

The distribution of reactedness is also sketched. Although it is not evident from Fig. 2, experience of other types of steady-flow combustion, together with study of the differential equations, makes it probable that as the mass flow rate is increased (for fixed pressure) the reactedness will steadily fall; at very high rates it is likely that the flame will be altogether extinguished. This matter is analysed in Section 9.2 below, and in Ref. 5.

2.7/

2.7 Differential equations: dimensionless form

As usual before computation, it is found convenient to simplify the equations by definition and substitution of dimensionless variables. A suitable set are:-

Droplet radius : $\zeta \equiv r/r_o$ ...(6)

Droplet velocity : $\chi \equiv \rho_g v/G$ ...(7)

Distance : $\xi \equiv R_o \rho_g x/Gr_o$ ...(8)

Vaporization rate : $\beta \equiv R/R_o$ ...(9)

Droplet drag : $S \equiv 9\mu_g/2R_o r_o \rho_\ell$ ...(10)

Gas velocity : $\omega \equiv \rho_g u/G$ ...(11)

Chemical loading : $L \equiv R_o \{c(T_b - T_u) + Q\}\rho_g / \dot{q}'''_m r_o$ ...(12)

where R_o = R with droplet in entry state and gas in equilibrium.

The differential equations thereupon take on the following forms:

(1): $$\chi \frac{d\zeta}{d\xi} = -\sigma \beta f_1 \qquad ...(13)$$

(2) and (4): $$\chi \frac{d\chi}{d\xi} = m \frac{Sf_2}{\zeta^2}\left[\frac{1-\zeta^3}{\delta} - \chi\right] \qquad ...(14)$$

(4): $$\omega = (1-\zeta^3)/\delta \qquad ...(15)$$

(5): $$\frac{d\tau}{d\xi} = \frac{1}{L}\cdot\frac{\psi}{(1-\zeta^3)} - 3\tau\sigma\frac{\zeta^2}{1-\zeta^3}\cdot\frac{\beta f_1}{\chi} \qquad ...(16)$$

In these equations, the independent variable is the distance, ξ. The dependent variables are ζ, χ, τ and ω. Of the remaining symbols, we have

$\sigma = \sigma(\tau)$ ...(17)

$\beta = \beta(\zeta, \chi - \omega)$ ...(18)

$m = m(\tau)$ ...(19)

$S =$ constant ...(20)

$C = C(\zeta, \chi - \omega)$ ...(21)

$\delta = \delta(\tau)$ ...(22)

$L =$ constant ...(23)

$\psi = \psi(\tau)$ ...(24)

f_1/

$$f_1 = f_1\left[\frac{\delta\zeta.|\chi - \omega|}{m}.Re_o\right] \qquad ...(25)$$

$$f_2 = f_2\left[\frac{\delta\zeta.|\chi - \omega|}{m}.Re_o\right] \qquad ...(26)$$

$$Re_o = 2Gr_o/\mu_g \qquad ...(27)$$

where all these functions and constants are supposed known. In addition, the solution will depend on the initial droplet injection velocity, χ_o.

2.8 Mathematical features of the problem

The equations (13), (14) and (16) form a set of simultaneous first-order differential equations. Moreover the boundary conditions ($\xi = 0 : \zeta = 1$, $\chi = \chi_o$, $d\tau/d\xi$ = finite) are all given at a single point. The problem is therefore one of straightforward numerical integration, for which many techniques are available.

Further, since ξ appears only in the denominator of the differential coefficients, division of (14) and (16) by (13), for example, ensures that only two equations have to be integrated simultaneously. The gas velocity, ω, can be evaluated from (15) after completion of the integrations.

It will be shown below that in simple cases (Model Ia) an analytical solution can be obtained.

3. Model I: Fast Reaction Rate

3.1 Nature of idealisation

When the chemical loading, L, is very small, examination of (16) and some thought about its physical significance reveal that the reactedness τ will be unity throughout: the gas phase is in equilibrium at all points. This occurs when the chemical reactivity of the gases is very large.

For bi-propellant systems, this means that the rate of burning is entirely determined by physical factors. For mono-propellants on the other hand, chemical reaction still influences the process because a flame propagates into the vapours streaming from the droplet surface and increases the temperature gradient at the surface.

It is probable that many rocket motors operate in the Model I régime.

3.2 Mathematical implications

Since $\tau = 1$, equation (16) no longer has to be considered. Moreover we can put $\sigma = 1$, $m = 1$, and $\delta = 1$. Equations (13), (14) and (15) can be correspondingly simplified.

3.3 Solution in terms of quadratures

Dividing (14) by (13), we obtain:

$$\frac{d\chi}{d\zeta} - \frac{3}{\beta\zeta^2}\frac{f_2}{f_1}.\chi = -\frac{S(1-\zeta^3)}{\beta\zeta^2}\frac{f_2}{f_1} \qquad ...(28)$$

wherein/

wherein it will be noted that the two functions of Reynolds number, f_1 and f_2, appear as a ratio. Now these functions represent respectively the increases in heat transfer and drag due to inertia effects close to the droplet. Examination of heat transfer and drag data for small spheres reveals that, for Reynolds numbers lower than 30, the ratio f_2/f_1 is equal to unity within about 6%. There is therefore little inaccuracy in assuming

$$\frac{f_2}{f_1} = 1. \qquad \ldots(29)$$

This approximation converts (28) into a linear differential equation, directly integrable by means of an integrating factor. (28) becomes

$$\frac{d\chi}{d\zeta} - \frac{S}{\beta\zeta^2}.\chi = -\frac{S(1-\zeta^3)}{\beta\zeta^2} \qquad \ldots(30)$$

in which of course S is a constant while β is a function of ζ alone. Its solution is

$$\chi = \exp\left[-S\int_{\zeta}^{'}(1/\beta\zeta^2)\,d\zeta\right]\left\{\chi_0 + S\int_{\zeta}^{'}\frac{(1-\zeta^3)}{\beta\zeta^2}\exp\left[S\int_{\zeta}^{'}(1/\beta\zeta^2)\,d\zeta\right]d\zeta\right\}. \qquad \ldots(31)$$

When the initial droplet velocity χ_0 is given, and S is known, evaluation of (31) gives the droplet velocity χ as a function of the droplet radius ζ.

The distance, ξ, for each ζ value can now be determined by evaluating the integral of equation (13), with σ equal to unity as before. We obtain

$$\xi = \int_{\zeta}^{'}(\chi/\beta f_1)\,d\zeta. \qquad \ldots(32)$$

This can be evaluated because χ is now a known function of ζ from (31), and ω is evaluable from (15) with δ put equal to unity, i.e.,

$$\omega = 1 - \zeta^3 \qquad \ldots(33)$$

f_1, the Reynolds number function, can now be inserted via (25) as a function of ζ. Re_0 needs to be given.

The length of the rocket motor necessary for the completion of combustion, ξ^* in dimensionless terms, is given by putting $\zeta = 0$ at the lower limit of (32).

4. Model Ia: Physically Controlled Vaporization Rate

4.1 Nature of the vaporization law

We now consider a particularly simple, but practically important, example of rockets in which the chemical reactivity is high but the droplet Reynolds number is so small that $f_1 = 1$. This is

a/

a particular example of the model I flame of Section 3.3 above. The system may be a bi-propellant one; or, if the fuel is a mono-propellant, then the droplets must be so small that the flames around them are relatively far from the surface. It is necessary that the droplets should be injected at their wet-bulb temperature.

This case is the well-known one in which the vaporization rate per unit surface area is inversely proportional to the droplet radius. This behaviour is expressed by

$$\beta = 1/\zeta. \qquad \ldots(34)$$

4.2 Solution of equations

For this case, equations (31) and (32) reduce to

$$\chi = [\chi_0 + 3/(S - 3)]\,\zeta^S + 1 - \zeta^3\, S/(S - 3) \qquad \ldots(35)$$

$$\xi = \frac{\chi_0 + 3/(S - 3)}{S + 2}.(1 - \zeta^{S+2}) + \tfrac{1}{2}(1 - \zeta^2) - \frac{S}{5(S - 3)}(1 - \zeta^S). \qquad \ldots(36)$$

Equation (33) also holds.

At the end of combustion, we therefore have

$$\zeta = 0: \quad \chi = 1 \qquad \ldots(37)$$

$$\omega = 1 \qquad \ldots(38)$$

$$\xi = \xi^* = (\chi_0 + 3S/10)/(S + 2). \qquad \ldots(39)$$

Equations (37) and (38) of course hold for all Model I flames at $\zeta = 0$ as a result of the definition of the quantities χ and ω. Equation (39) is the interesting one, for it enables the minimum length of rocket motor, x^*, to be evaluated.

For the particular case in which $S = \infty$ (very large gas viscosity), the droplet velocity, χ, always equals the gas velocity, ω. The solution simplifies to

$$\chi = \omega = 1 - \zeta^3 \qquad \ldots(41)$$

$$\xi = \tfrac{3}{10} - \tfrac{1}{2}\zeta^2 + \tfrac{1}{5}\zeta^5 \qquad \ldots(42)$$

$$\xi^* = \tfrac{3}{10}. \qquad \ldots(43)$$

4.3 Graphical representation of results

Equation (39) has been evaluated. ξ^* is plotted versus S in Fig. 3 for various values of χ_0. It will be used below for determining the minimum permissible length of rocket motor.

Equations (33), (35) and (36) have also been evaluated for various combination of values of χ_0 and S. Fig. 4 shows a

set/

set of curves for $\chi_o = \frac{1}{2}$ and $S = 1$, which are believed to be values representative of rocket practice. These curves give the variation with distance ξ of the droplet velocity χ, the gas velocity ω, and the droplet radius ζ.

Figs. 5, 6, 7, 8 and 9 give results for $S = 0, 0.5, 1, 2,$ and ∞. The ζ, ω and χ curves are plotted on separate graphs. Values of χ_o equal to 0, 0.5, 1.0, 1.5 and 2.0 have been considered.

The physical significance of the graphs is discussed below.

5. Discussion of the Model Ia Results

5.1 The significance of S

From equation (10) and the definition of R, we have

$$S = \frac{9\mu}{2r_o\rho_\ell}\frac{\zeta}{(k/c\rho_\ell)\ell n(1+B)}\frac{r_o}{} = \frac{9Pr}{2\ell n(1+B)} \qquad \ldots(44)$$

where Pr is the Prandtl number of the gas and mean values of the transport properties are used.

If, as is reasonable, the droplet drag is reduced below its Stokes Law value by outward mass transfer from the surface in the ratio $(1/B)\ell n(1+B)$, equation (44) can be corrected to

$$S = \frac{9Pr}{2B}. \qquad \ldots(45)$$

Now, for all gases, Pr is about 0.7. The transfer number B varies with the gas and liquid properties but is of the order of 6 for bi-propellants, and somewhat lower for mono-propellants. We conclude that S is of the order of 0.5. This value is included among those used in the calculations; other values have been covered in order to exhibit the trends.

5.2 The significance of ξ^*; relation to L^*

From equation (8) and the definition of R, we have

$$\xi^* = x^*\rho_g\frac{(k/c\rho_\ell)\ell n(1+B)}{Gr_o^2}. \qquad \ldots(46)$$

With ξ^* known from Fig. 3, and other quantities given among the design data, equation (46) can be used to permit calculation of x^*, the minimum length of rocket motor for complete combustion.

It is evident that, other things being equal, x^* is proportional to G; i.e., the greater the mass flow per unit cross-sectional area, the longer the combustion chamber must be. This means that there is a maximum permissible mass flow per unit volume.

This/

This fact underlies the use of the characteristic length, L*, to specify rocket motor conditions. Since

$$L^* = Ax^*/A_t \qquad \ldots(47)$$

where A = motor cross-sectional area

A_t = throat cross-sectional area,

and since from the theory of one-dimensional compressible isentropic flow

$$\frac{A}{A_t} = \frac{1}{M}\left[\frac{2\left(1 + \frac{\gamma-1}{2}M^2\right)}{\gamma+1}\right]^{\frac{\gamma+1}{2(\gamma-1)}} \qquad \ldots(48)$$

where γ = ratio of specific heats of the gas (assumed constant)

M = Mach number of fully burned gases in combustion chamber

$= G/\rho_g a$

a = sonic velocity of gases in combustion chamber,

we have,

$$L^* = x^* \frac{a\rho_g}{G}\left[\frac{2\left\{1 + \frac{\gamma-1}{2}(G/\rho_g a)^2\right\}}{\gamma+1}\right]^{\frac{\gamma+1}{2(\gamma-1)}}$$

$$= \frac{\xi^* a r_o^2 [\{2/(\gamma+1)\}\{1 + (\gamma-1)(G/\rho_g a)^2/2\}]^{\frac{\gamma+1}{2(\gamma-1)}}}{(k/c\rho_\ell)\ell n(1+B)}. \qquad \ldots(49)$$

Equation (49) permits L* to be evaluated from the properties of the propellants and the injected droplet radius r_o. In addition it is necessary to know ξ^*, which depends, as Fig. 3 shows, on S and χ_o. S is established from the considerations discussed in Section 5.1; χ_o is the ratio of droplet injection velocity to final gas velocity in the combustion chamber, and may therefore also be assumed known. The expression $(G/\rho_g a)^2$ in equation (49) will often be sufficiently small to be neglected.

5.3 Example of the calculation of L*

The following data may be taken as representative of many rocket motors:-

$$a = 3000 \text{ ft/sec}$$

$$r_o = 0.005 \text{ cm}$$

$$(k/c\rho_\ell)\ell n(1+B) = 2 \times 10^{-3} \text{ cm}^2/\text{sec}$$

$$[\{2/(\gamma+1)\}\{1 + (\gamma-1)(G/\rho_g a)^2/2\}]^{\frac{\gamma+1}{2(\gamma-1)}} = 0.6$$

$$\xi^* = 0.2 \quad \text{(from Fig. 3 with } S = 0.5,\ \chi_o = 0.3).$$

Hence/

Hence we obtain

$$L^* = 0.2 \times 3000 \times (0.005)^2 \times 0.6/2 \times 10^{-3}$$

$$= 4.5 \text{ ft} = 54 \text{ inches.}$$

This is of the order of magnitude encountered in practice. Although more detailed examination of particular cases is necessary, we can already conclude that it is possible that the theoretical Model Ia is capable of representing practical rocket performance reasonably well.

5.4 Discussion of gas and droplet velocity distributions

Taking Fig. 4 as typical, we see that the droplet velocity χ at first decreases as a result of the drag exerted by the gas. However the gas velocity ω increases as a result of vaporization and burning (indicated by the decrease in droplet radius ζ). Eventually the gas velocity exceeds that of the droplet; the drag now tends to accelerate the latter. The droplets only succeed in "catching up with" the gas at the last moment however, namely at ξ^* where ζ has just become zero.

Figs. 5 to 9 illustrate the way in which the values of S and χ_0 affect the velocity distributions. In Fig. 5, where $S = 0$, the droplet velocity is unaffected by drag, so $\chi = \chi_0$ throughout. In Fig. 9, the other extreme case, where $S = \infty$, drag is so great that the droplets and gas have the same velocity whatever the value of χ_0. Figs. 6, 7 and 8 illustrate more realistic conditions. It will be recalled that in practice S is likely to vary between 0.5 and 1.

For a fixed value of S, the graphs show that ξ^*, the quantity entering the expression for L^*, always increases with χ_0. This means of course that droplets which are injected at high speed penetrate far downstream before burning, requiring a long combustion chamber. The Model Ia theory leads to the practical conclusion that the injection velocity ought to be small. However considerations of chemical reaction rate indicate a limit to this (Model II theory, Ref. 5) (see also Section 9.2 below). In practice χ_0 probably varies between 0.1 and 0.5.

5.5 Summary of factors influencing L^*

Equation (49) and Fig. 3 provide the information from which we can deduce what can be done to make L^* small:-

(i) ξ^* should be small. This depends only on χ_0 and S (Fig. 3). S is not in the designer's control, but χ_0 is. It should be small.

(ii) B should be large. This means that the fuels should have large heat of reaction and small latent heat of vaporization. They should be injected at this adiabatic vaporization temperature; this usually means that they should be heated between leaving the fuel tanks and entering the injector.

(iii) The injected droplet radius should be small, for L^* is proportional to the square of the initial droplet size. Although not dealt with explicitly by the foregoing theory, we can be certain that, if the droplets are not of uniform size on entry, it is the largest ones which control L^*.

(iv)/

(iv) $G/\rho_g a$, i.e., the Mach number of the gases in the combustion chamber just before entering the nozzle, should preferably be much less than unity; for then this term, which in any case is of secondary importance, vanishes entirely. One may conclude that short fat chambers can have a somewhat smaller L^* than long thin ones. The effect is not straightforward however, for χ_0 may increase as $G/\rho_g a$ is decreased.

(v) a, γ and $(k/c\rho_\ell)$ are usually not under the designer's control, and in any case vary comparatively little from one propellant system to another. Moreover for a given gas ac/k is almost independent of temperature.

6. The Effect of Droplet Reynolds Number

6.1 Model Ia at larger Reynolds numbers

In the above calculations it was found convenient to put $f_1 = 1$, this involved assuming that Stokes's Law held for drag and that the Nusselt number of the droplet was 2. We now consider the error involved in this assumption. It is convenient still to assume Reynolds Analogy, namely $f_1 = f_2$; for f_1 we take the Frössling[6] equation, which in the present notation becomes, for $Pr = 0.7$,

$$f_1 = 1 + 0.245\, Re_0 . |\omega - \chi| . \zeta \qquad \ldots(50)$$

where Re_0 is obtained from (27).

6.2 Results for $\chi_0 = \frac{1}{2}$, $S = 1$

Equations (33) and (35) are unaffected by the new expression for f_1. Equation (36) must be replaced however by the quadrature expression (36).

Equation (36) has been evaluated for the case $\chi_0 = \frac{1}{2}$, $S = 1$ for three values of Re_0, namely 10, 100 and 1000. The corresponding curves for ζ, ω and χ versus ξ are plotted in Fig. 10a, b and c. These curves should be compared with those of Fig. 4.

6.3 Discussion

Comparison shows that the main effect of increasing Re_0 is to reduce the horizontal scale of the diagrams. The corresponding values for ξ^* are shown in Table 1.

Table 1

Re_0	0	10	100	1000
ξ^*	0.267	0.21	0.147	0.077

Values of Re_0 in practical rockets vary considerably, but they are likely to be of the order of 100 in many cases. We see that consideration of this effect may yield a ξ^*, and so an L^*, of only one half the value obtained if the Reynolds number is assumed small.

7./

7. Residence-Time Calculations

7.1 Purpose

It has been suggested that the processes occurring inside rocket motors might be investigated experimentally by injecting a momentary pulse of tracer material into the fuel line; the variation of the tracer concentration in the exhaust gases would then be measured. In order to aid in interpreting such diagrams, it is interesting to see what concentration-time curves are to be expected for Model Ia flames.

7.2 ξ-θ diagrams

Since the droplet and gas velocities have been calculated as functions of position ξ, it is merely a matter of integration to calculate and plot the paths of droplets and gas particles on a distance-time (ξ-θ) diagram.

We obtain that the dimensionless time θ_ℓ which a droplet takes to reach the position ξ from the injector face is given by:-

$$\theta_\ell = \tfrac{1}{2}(1 - \zeta^2) \qquad \ldots(51)$$

where, of course, ζ is obtainable, for low Re, from (36). θ is related to real time t by

$$\theta = R_0 t / r_0 . \qquad \ldots(52)$$

The time θ_g spent by the gas between position ξ and the exit is given by

$$\theta_g = \int_0^\zeta \frac{\chi \zeta d\zeta}{1 - \zeta^3} \qquad \ldots(53)$$

the evaluation of which in terms of ξ requires both (35) and (36).

Equations (51) and (53) have been used to construct Fig. 11(a) which shows a single droplet path and several gas particle paths on an ξ-θ diagram for the Model Ia case, $\chi_0 = \frac{1}{2}$, $S = 1$.

It is seen that the droplet at first overtakes gas particles, is later overtaken by them, and finally travels along with them. In particular it will be noted that the gas particles take an infinite time to travel the whole distance from the injector to the outlet ($\xi = \xi^*$), because of their very low velocities near the injector.

7.3 Residence-time distribution

Values of ζ^3 (0.9, 0.8, ... 0.1) are marked at appropriate places on the droplet path. These indicate the proportion of initial droplet mass still in the liquid phase.

An element of the droplet at first travels along the droplet path, and then, on vaporization, travels along the gas particle path. The outer layers of the droplet "peel off" first. Thus the layer at radius $\zeta = \sqrt[3]{0.9}$ travels with the droplet to the point marked $\zeta^3 = 0.9$ and then enters the gas.

These considerations have been used to construct Fig. 11(b), showing C (= concentration of tracer at ξ^*) versus θ, which is

plotted/

plotted with C horizontal on the right. It is evident that, for a time $\theta = 0.41$ after injection of the tracer, C is zero; thereafter the tracer concentration rises suddenly to a peak followed by a slow fall-off. Between $\theta = 0.41$ and $\theta = 0.5$, the time at which the droplet arrives, the tracer concentration consists of two contributions, one having vaporized early, the other late; from $\theta = 0.50$ onwards, only tracer from the outer layers of the droplet appears.

We may conclude that, even in the absence of turbulent mixing in a streamwise direction, and in the absence of recirculation, the differing velocities of droplet and gas ensure a wide spread in the residence times of elements of a tracer pulse.

It would of course be interesting to test this consequence experimentally. Whether the technique can be used to confirm the validity of the present view of rocket combustion depends however on what residence-time distributions are to be expected from other combustion mechanisms. Such distributions have not yet been examined. However it can be stated that if intense turbulence were dominant, the residence-time distribution would be much more symmetrical than that of Fig. 11(b).

7.4 Time-lag

Some theories of low-frequency rocket motor oscillation make use of the concept of a "time-lag" between injection and combustion. The present theory throws light on this concept. Inspection of Fig. 11(a) shows, for the Model Ia case $\chi_0 = \frac{1}{2}$, $S = 1$, the relation between time from injection θ and fraction unvaporized ζ^3. Assuming, as has been done above, that the reaction rate is very high, the fraction burned is $1 - \zeta^3$. Fig. 12 shows a plot, for the case of Fig. 11, of time of burning versus fraction burned.

It is evident that the burning is spread out over a dimensionless time of $\theta = 0.5$. One half of the droplet has burned however after a time of $\theta = 0.13$. For simple theories this might be assumed to be the average time lag. Inspection of equation (52) and the definition of R shows that, in real terms, the time lag is proportional to the inverse square of the droplet radius for Model Ia rockets.

It should be observed that there is no direct relation between the above average time-lag and the residence-times measured by the tracer technique.

8. Relation of Present Work to that of Priem[7,8]

Since the present work was begun, two reports by Priem have become available which proceed along similar lines. The following similarities and differences may be noted.

8.1 Similarities

Priem postulates a model which is essentially the same as Model I of the present paper. Reynolds number effects are considered, but chemical reaction is not. The results are expressed in the form of curves of droplet size and velocity, gas velocity, etc., versus distance.

8.2 Differences

The main feature in which Ref. 7 goes beyond the present work is in taking account of transient effects in the droplet, i.e., in

supposing/

supposing that the liquid is injected below that of adiabatic vaporization. It is shown that this considerably reduces the rate of vaporization in the regions close to the injector.

Priem solves his equations numerically by means of a high-speed computing machine. The equations are not expressed dimensionlessly, so the solutions can only be used for the particular droplet sizes, fuels, and injection conditions for which integrations have been carried out. n-heptane was the fuel, burning in oxygen; the latter is supposed, implicitly, to have the same physical properties as heptane.

In Ref. 8, Priem considers the case in which not all the heptane droplets have the same initial radius. The calculations show that, as may be expected, the minimum combustion chamber length is controlled by the larger droplets in the injected spray.

8.3 Comparison

Priem's work has shown that transient effects are important. In the present method these can be accounted for by introducing the appropriate $\beta(\zeta)$ function. Such solutions will be reported in a later paper. Priem's treatment of non-uniform sprays marks a definite step forward.

In the author's opinion, the use of dimensionless variables is an advantage of the present formulation; it increases generality, permits trends to be perceived, and eases the calculations. The present calculations have been performed with a desk calculating machine.

9. Further Work to be Done

9.1 Examination of actual rocket data

If the foregoing theory is to be useful, a detailed study of actual rocket combustion must be made in its light. There are three parts to this:-

(i) Collection of data on droplet sizes, injection velocities, final gas velocities, latent heats of fuel vaporization, heats of reaction, etc., for practical fuels and injectors.

(ii) Insertion of these data in the above theoretical relations, leading to predictions of L*, residence-time distribution, pressure distribution, etc.

(iii) Comparison of these predictions with the experimental performance of the corresponding rocket motors, and subsequent refinement of the theory to make agreement better.

9.2 Further theoretical work

More Model I flames need to be investigated, particularly with the $\beta(\zeta)$ relations appropriate to mono-propellants[1], and those valid for fuels of initially low temperature. It may be possible, as a result of such studies, to explain the markedly different L* values of current bi-propellant and mono-propellant rockets and also to provide rules for the designer.

Model II flames need to be investigated in order to establish the rôle of chemical reaction in rocket motors. That there is such an influence can be ascertained by inspecting equation (16) for the neighbourhood of the injector ($\zeta = 1$). We find that unless the

chemical/

chemical loading L is less than about $\chi_o/2$, the flame will be extinguished. Now combining the definition (12) of L with the definition of R_o, we have as a condition for existence of a flame:

$$\frac{k\rho_g}{c\rho_\ell} \frac{(c\overline{T_b - T_u} + Q)\ell n(1+B)}{\dot{q}'''_m r_o^2} < \frac{\chi_o}{2}. \qquad \ldots(54)$$

It appears that very small droplets, coupled with low injection velocity, may succeed in extinguishing the flame. It is necessary to examine, in the light of available reaction-rate data, whether this condition is in practice easily or only just fulfilled.

It should be emphasised that only steady combustion has been considered. However the one-dimensional model may in time prove helpful in the study of unsteady phenomena as well.

10. Conclusions

(a) A one-dimensional theoretical model of a liquid fuel rocket motor has been set up, taking account of droplet motion, gas motion, droplet disappearance, and chemical reaction.

(b) The equations are simultaneous first-order differential equations presenting no serious mathematical difficulty. With some simplifications, which are believed to be realistic for many practical cases, analytical solution is possible.

(c) When chemical reaction is very rapid, the L* of a propellant system is chiefly determined by the size and velocity of the injected droplets. An explicit formula is given, permitting calculation of L*.

(d) The main need now is for collection of the appropriate data for injectors and fuels, the insertion of these data in the theoretical equations, and the comparison of the predictions with experiment.

Acknowledgements

The author gratefully acknowledges the help of Miss M. P. Steele, who did the calculations and drew the graphs.

References/

References

No.	Author(s)	Title, etc.
1	D. B. Spalding and V. K. Jain	Theory of the burning of mono-propellant droplets. C.P.No.447. May, 1958.
2	D. B. Spalding	Progress in flame theory. AGARD Combustion and Propulsion Colloquium, March, 1958.
3	O. A. Saunders and D. B. Spalding	A.S.M.E./I.Mech.E. Joint Combustion Conference, 1955, p.23.
4	Deleted	
5	J. Adler	A one-dimensional theory of liquid-fuel rocket combustion II: The influence of chemical reaction. Communicated by Dr. D. B. Spalding. C.P.No.446. May, 1958.
6	N. Frössling	Beitr. Geophys. 52 (1938) 170.
7	R. J. Priem	Propellant vaporization as a criterion for rocket engine design; calculations of chamber length to vaporize a single n-heptane drop. N.A.C.A. Technical Note 3985. July, 1957.
8	R. J. Priem	The propellant vaporization as a criterion for rocket-engine design; calculations using various log-probability distributions of heptane drops. N.A.C.A. Technical Note 4098. October, 1957.

FIGS. 1 & 2

FIG. 1.

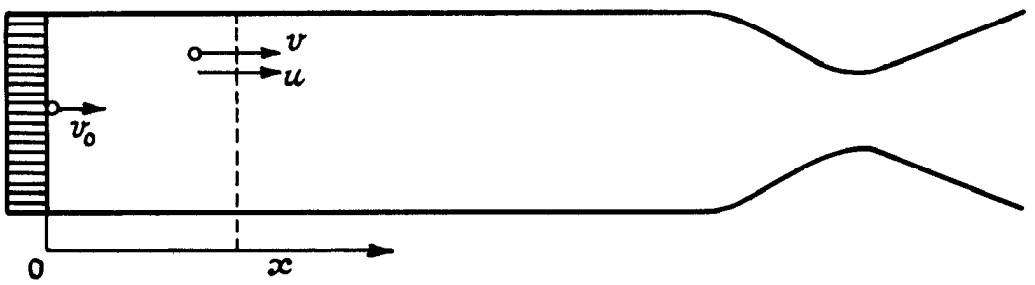

Model liquid-fuel rocket motor

FIG. 2.

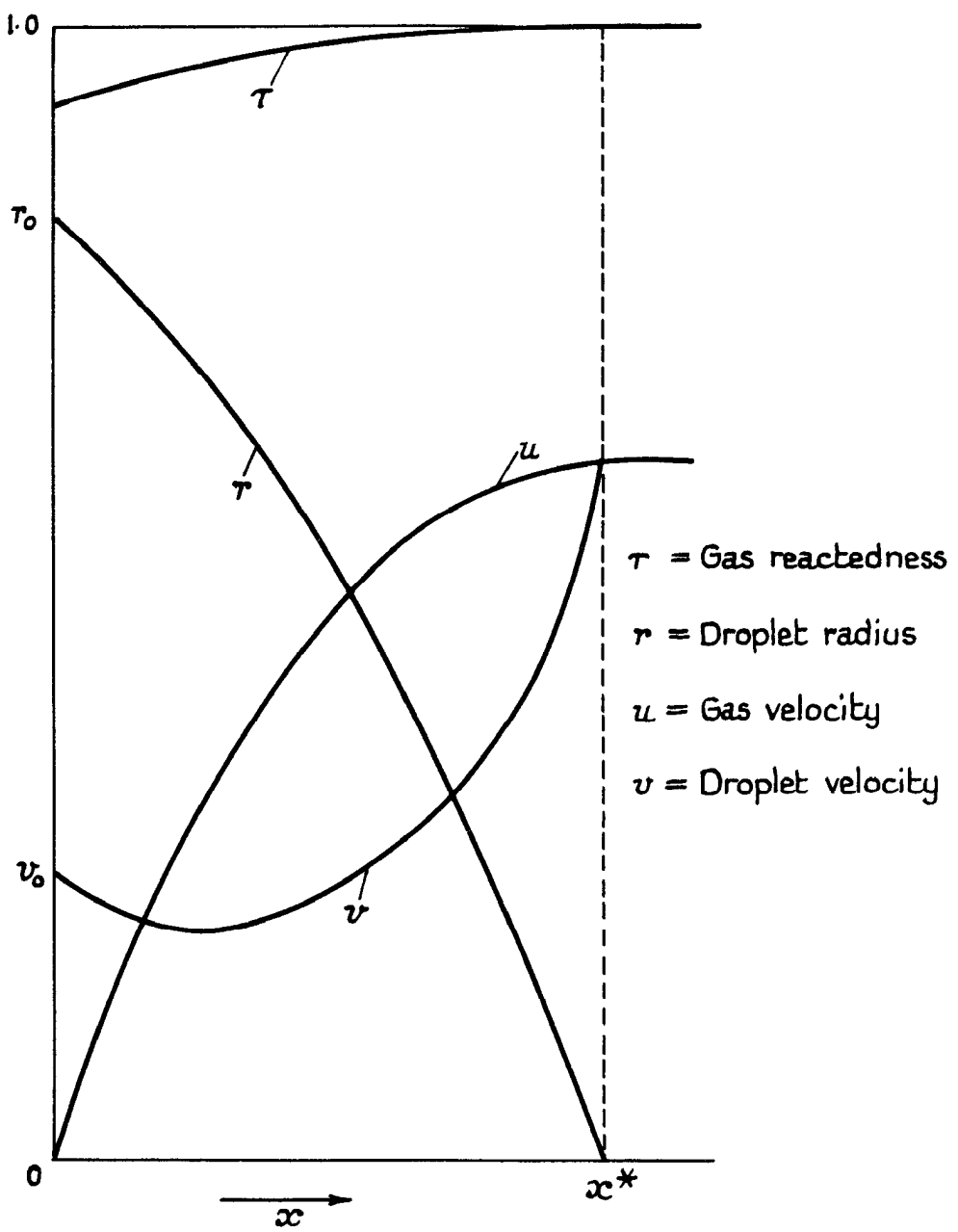

Variation of droplet and gas conditions along length of model rocket motor

Fig 3 & 4

Fig. 3.

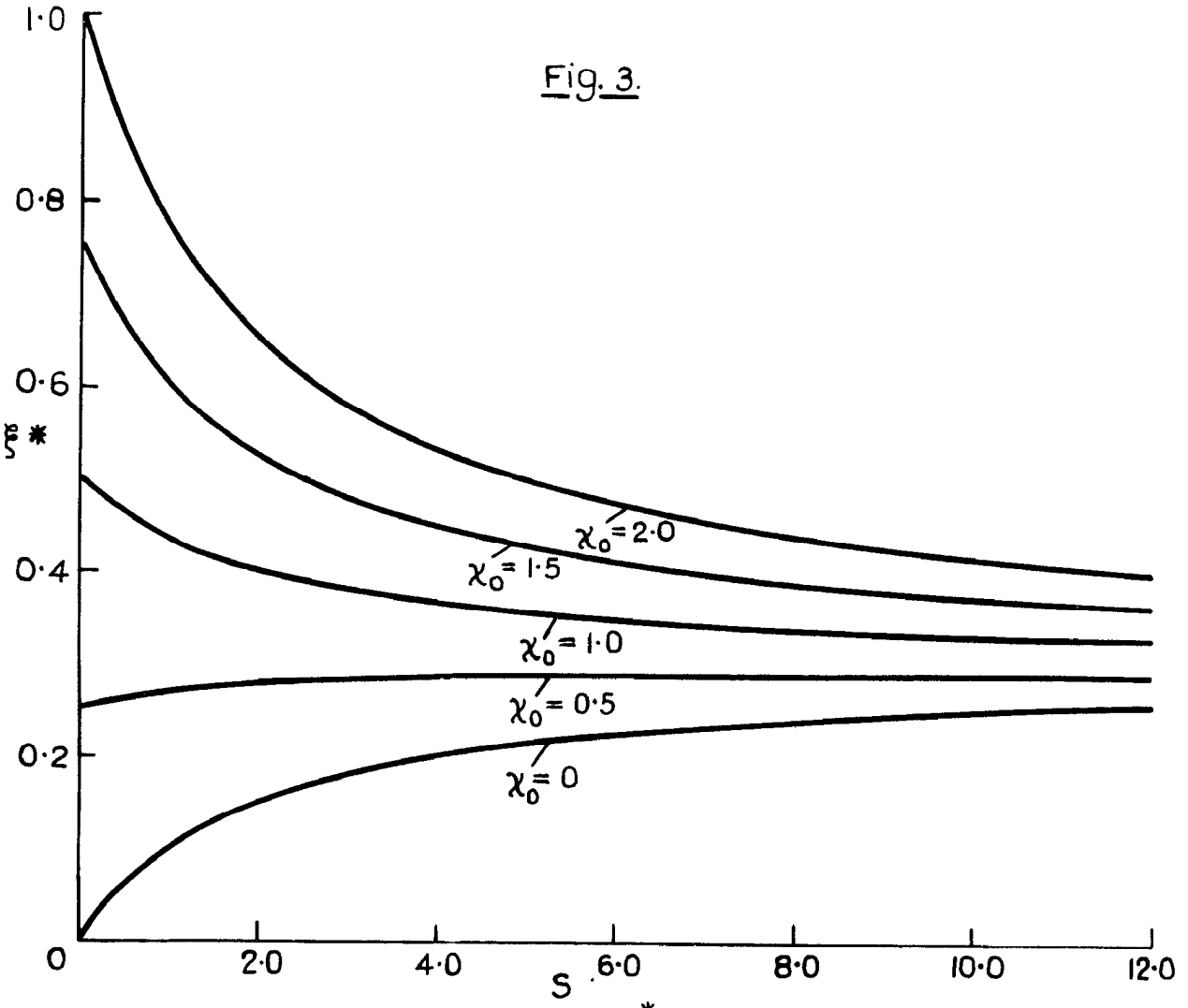

Minimum length of rocket motor ξ^*; influence of χ_0 and S for model Ia.

Fig. 4.

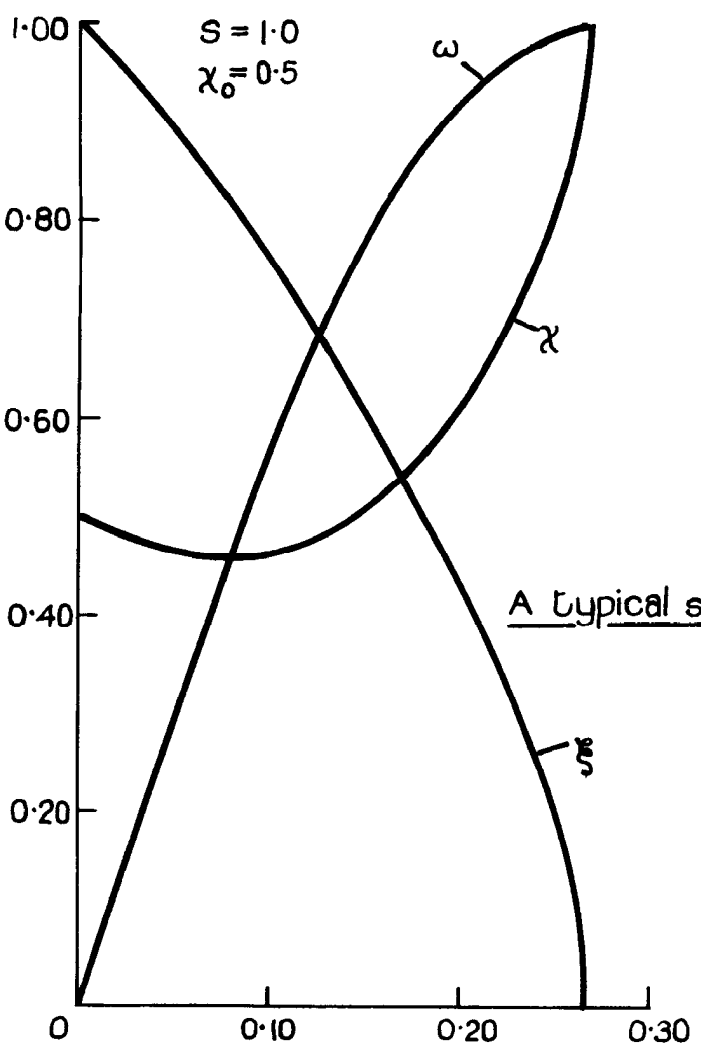

A typical solution for a model Ia rocket.

FIG. 5.

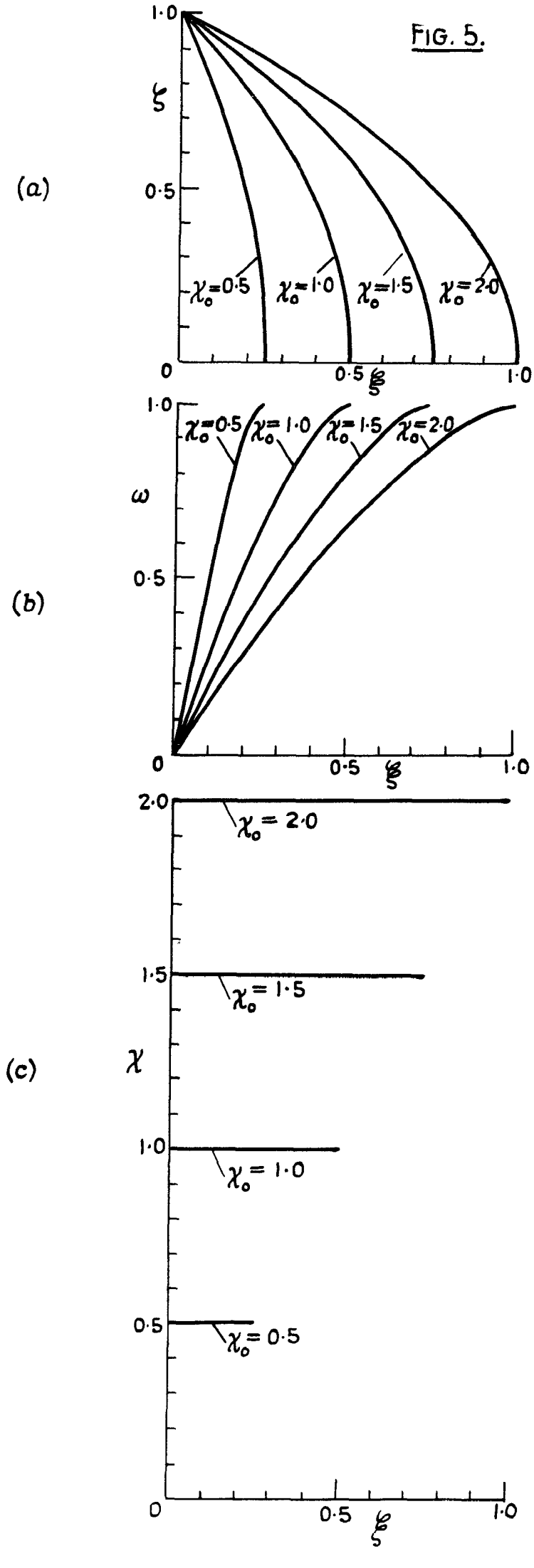

Model I a solutions; $S = 0$.

FIG. 6.

FIGS. 6 & 7.

FIG. 7.

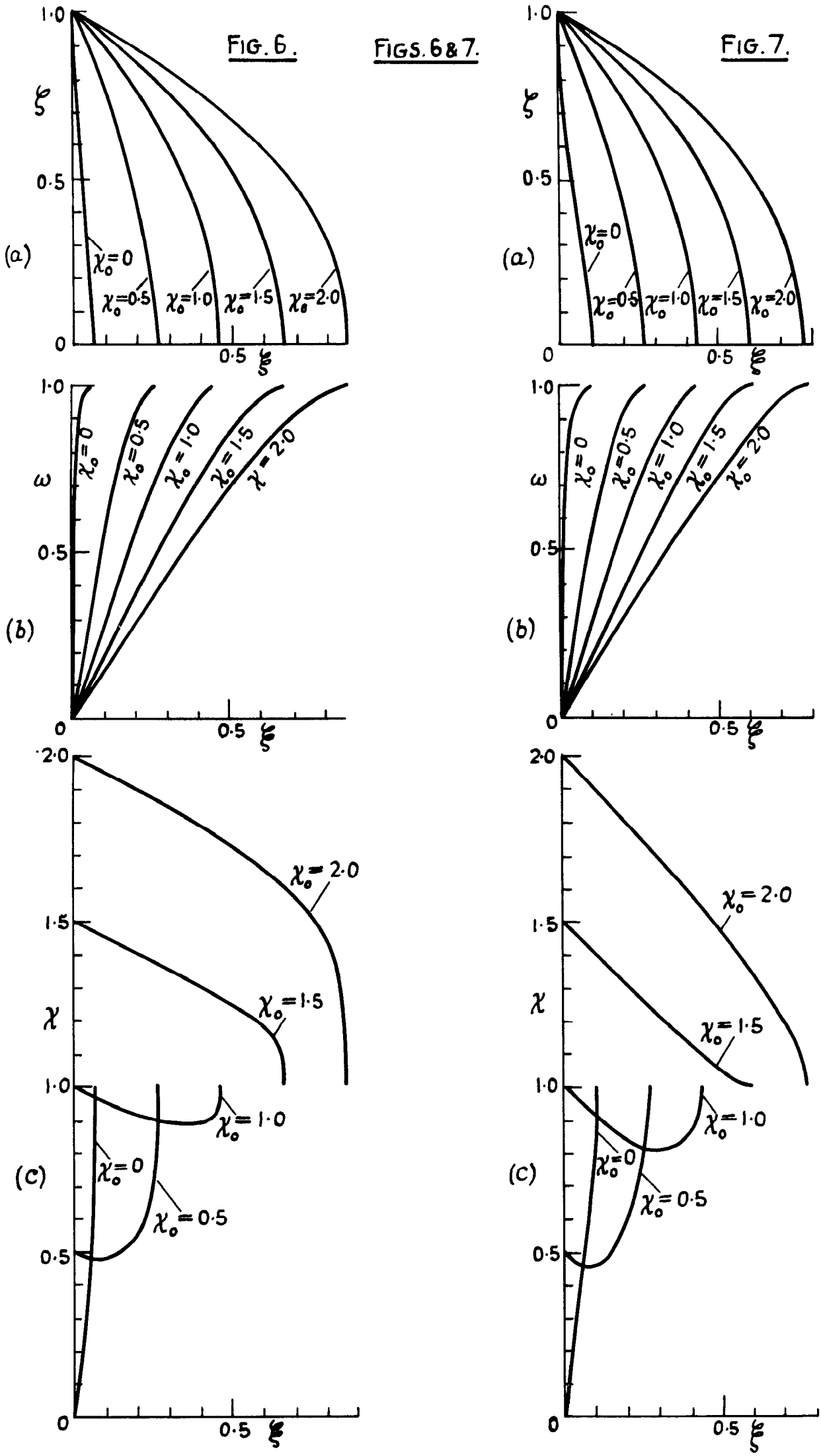

Model I a solutions; S = 0·5

Model I a solutions; S = 1·0

Fig. 8 & 9.

Fig. 8.

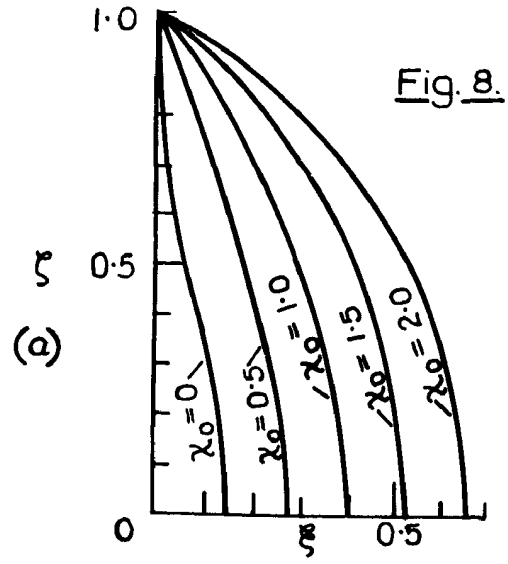

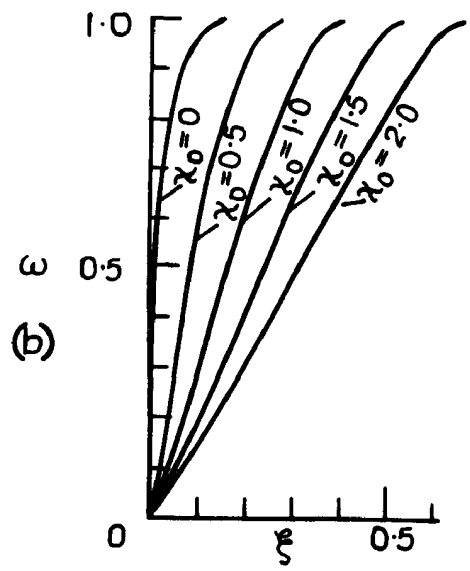

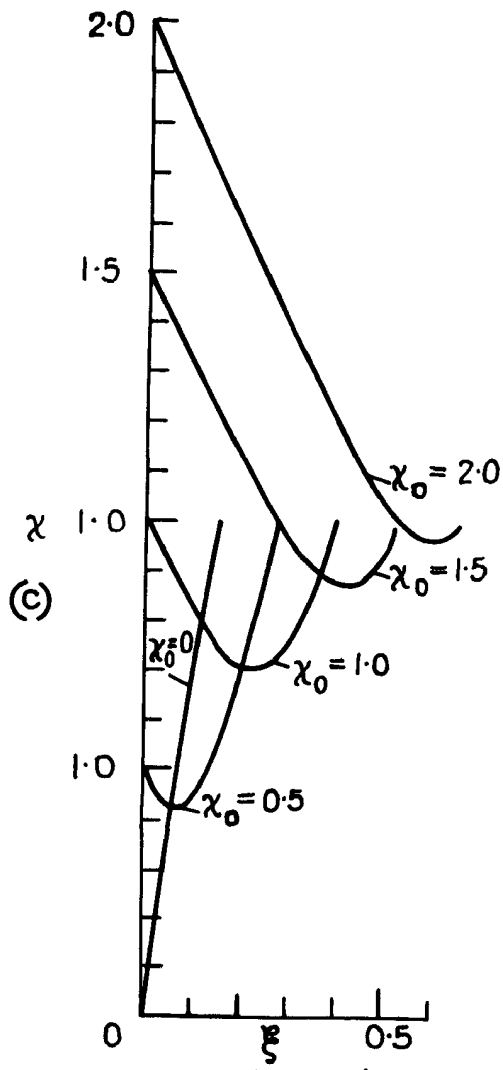

Model Ia solution, S = 2·0

Fig. 9.

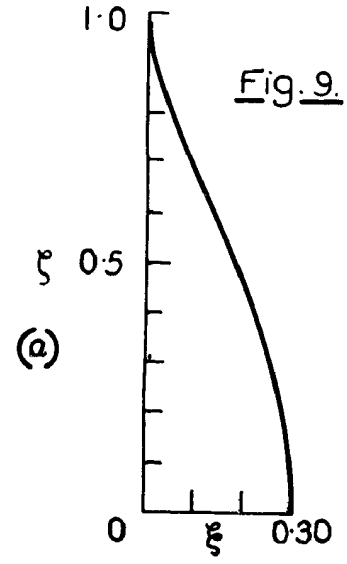

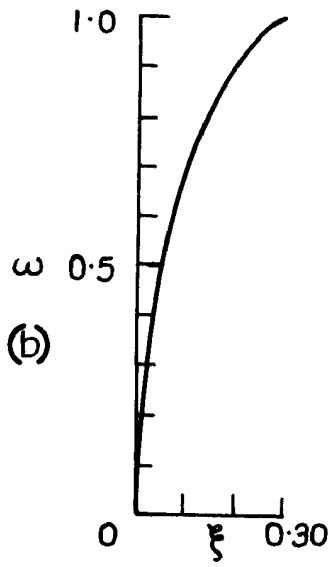

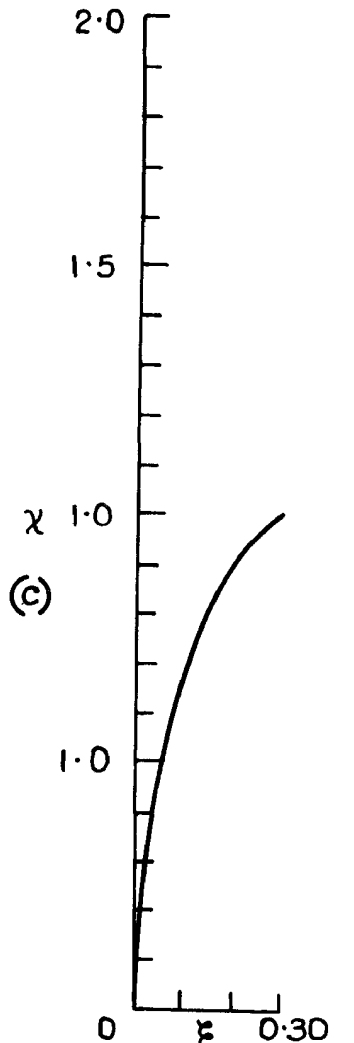

Model Ia solution S = ∞

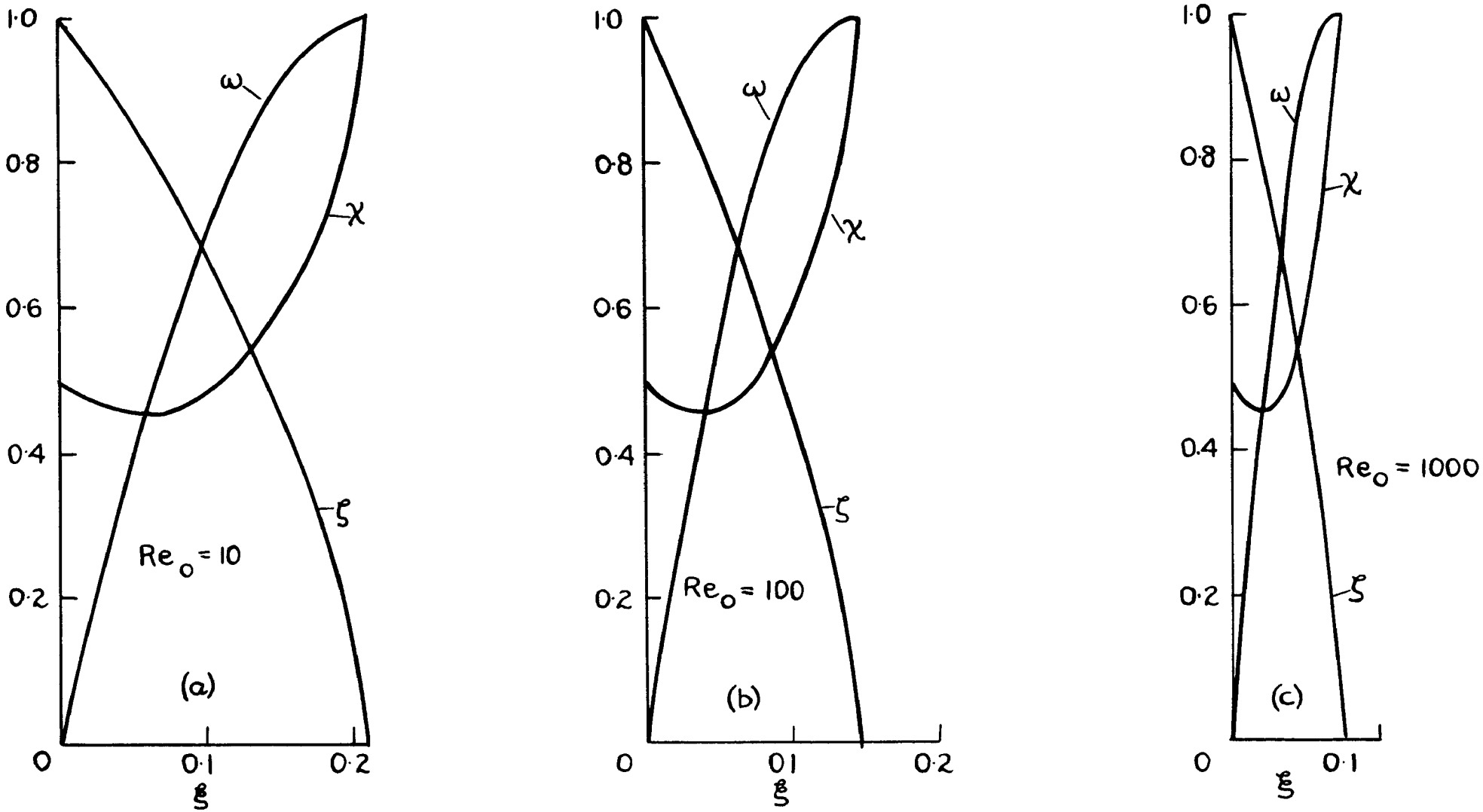

FIG 10(a),(b)&(c).

Effect of droplet Reynolds number on model I a. rocket, for $\chi_0 = 0.5$, $S = 1$. Graphs should be compared with Fig. 4., which represents $Re_0 = 0$.

FIG. 11 (a) & (b)

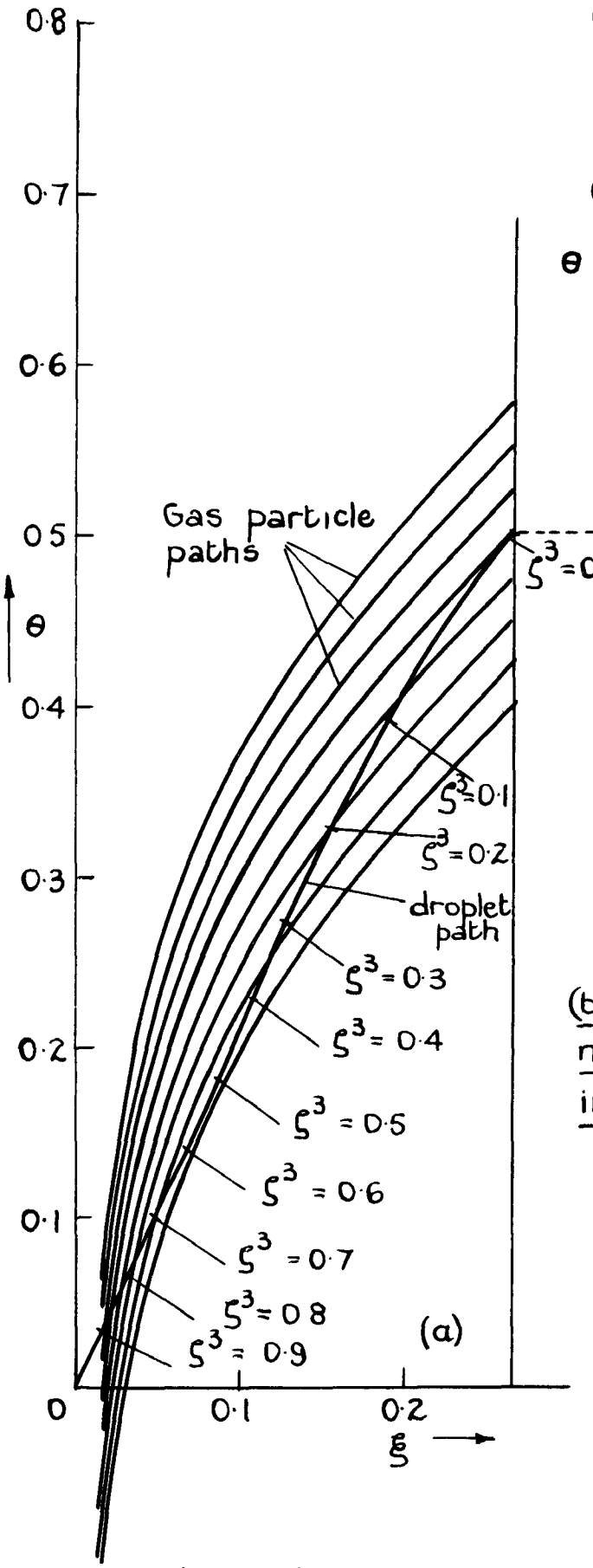

(a) Droplet and gas particle paths on distance - time (ξ - θ) graph, for $\chi_0 = 1/2$, $S = 1$, model I a.

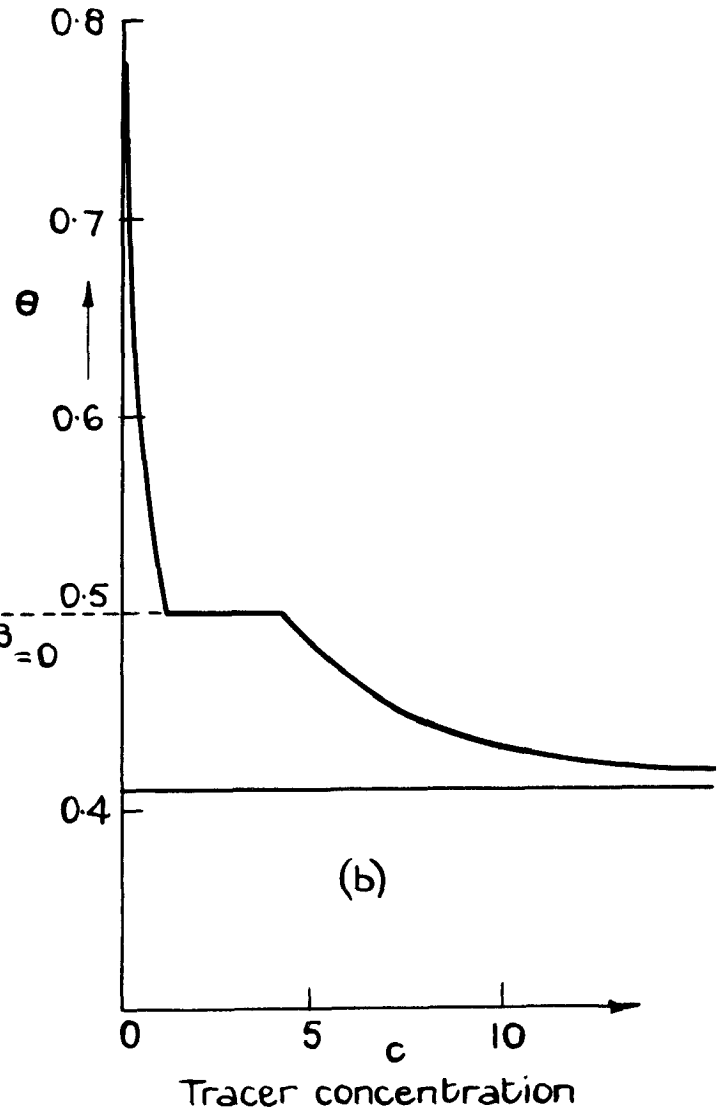

(b) Tracer concentration at outlet nozzle versus time from tracer injection for same rocket motor.

FIG. 12.

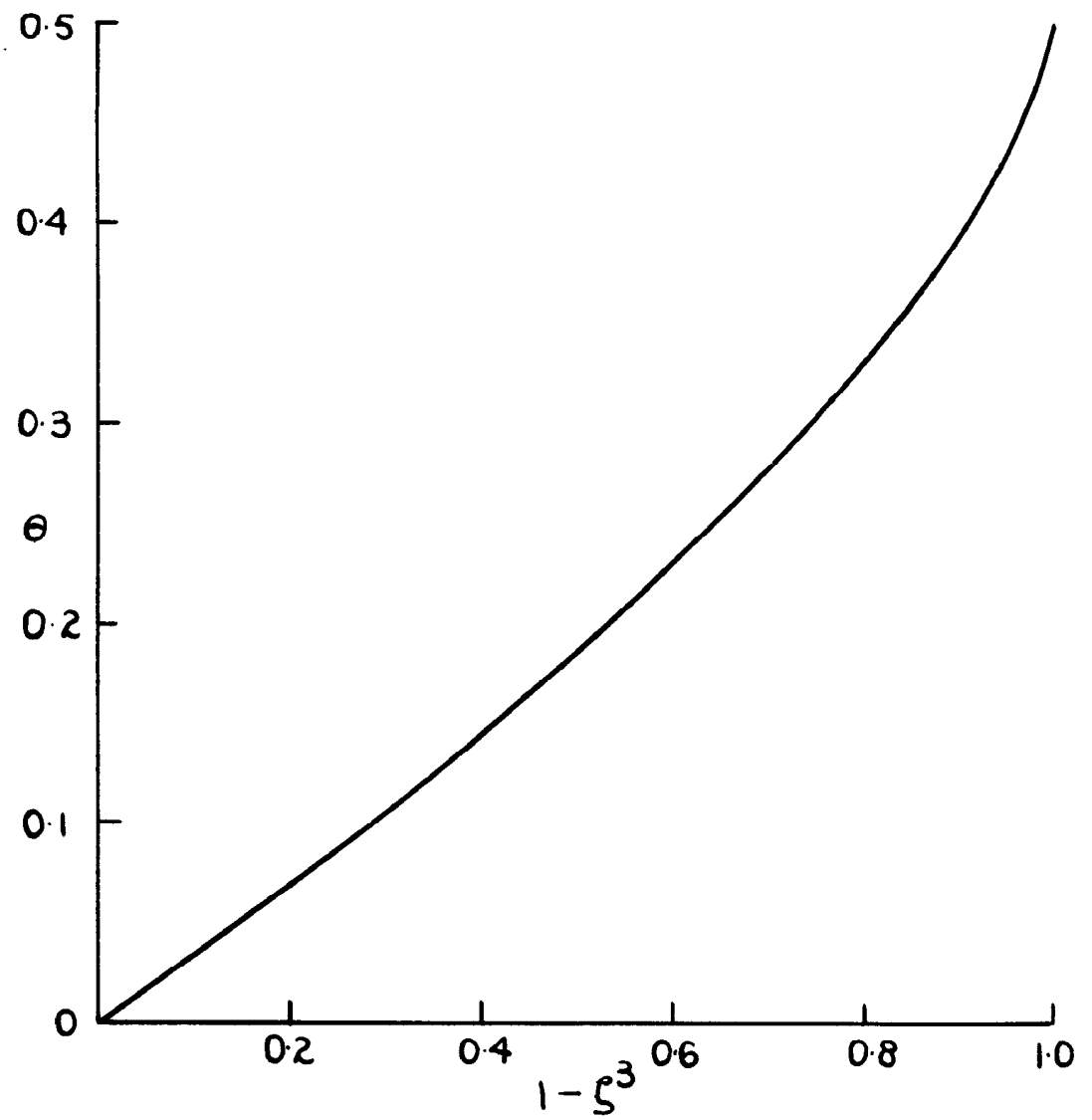

Time of burning versus fraction burned:
Model I a, $\chi_0 = 1/2$, $S = 1$.

C.P. No. 445
(20,175)
A.R.C. Technical Report

Printed and published by
HER MAJESTY'S STATIONERY OFFICE

To be purchased from
York House, Kingsway, London W.C.2
423 Oxford Street, London W.1
13A Castle Street, Edinburgh 2
109 St Mary Street, Cardiff
39 King Street, Manchester 2
Tower Lane, Bristol 1
2 Edmund Street, Birmingham 3
80 Chichester Street, Belfast
or through any bookseller

Printed in Great Britain

S.O. Code No. 23-9011-45

C.P. No. 445